


## Article

# Impact of Groundwater Fluctuations on the Stability of Super-Large-Diameter Caissons before and after Reinforcement

Leisi Dou <sup>1</sup>, Haitao Wang <sup>2</sup>, Bin Li <sup>3,\*</sup> , Yulin Yang <sup>3</sup> and Danyang Di <sup>3</sup>

- <sup>1</sup> Zhengzhou Municipal Zhongyuan District Agriculture Rural Work Committee, Zhengzhou 450006, China; 18810519211@163.com
- <sup>2</sup> Zhengzhou Zhengfa Water Conservancy Engineering Co., Ltd., Zhengzhou 450006, China; hotiler@sina.com
- <sup>3</sup> School of Water Conservancy and Transportation, Zhengzhou University, Zhengzhou 450001, China; 13513563638@163.com (Y.Y.); danyangdi@zzu.edu.cn (D.D.)
- \* Correspondence: 13523519067@163.com

**Abstract:** Super-large-diameter caissons, serving as working wells for trenchless pipe jacking technology, are being extensively constructed alongside the increasing adoption of trenchless technology in urban areas. However, being regarded merely as ancillary structures, the structural stability of a caisson during both construction and operation phases are often neglected. This study, centered on the super-large-diameter caissons within the Jinshui River flood control project in Zhengzhou, China, systematically monitored the mechanical behavior of caisson structures and surface settlement during construction and operational phases. Utilizing a validated FE method, the influence of groundwater fluctuations on the structural stability of caissons during operational phases was examined. Furthermore, potential occurrences of loose soil, voids, and caisson tilting were considered. Subsequently, the applicability of permeable polymer, foam polymer, and anchor rod reinforcement techniques were evaluated, followed by an analysis of the structural stability of the caissons post reinforcement during long-term operations. The findings demonstrate the minimal horizontal displacement of and stress variation in caissons under seasonal groundwater fluctuations, without significant structural alterations. Nevertheless, the presence of loose soil, voids, and caisson inclinations may decline the caisson's support force and bearing capacity. With the increase in non-compactness, void size, and inclination, the structural stability of caissons notably diminishes. Reinforcing loose soil with permeable polymers, filling voids with foam polymers, and utilizing anchor rods are all effective methods for strengthening caisson structures and enhancing their stability.

**Keywords:** super-large-diameter caissons; trenchless technology; groundwater fluctuations; structural stability; reinforcement



**Citation:** Dou, L.; Wang, H.; Li, B.; Yang, Y.; Di, D. Impact of Groundwater Fluctuations on the Stability of Super-Large-Diameter Caissons before and after Reinforcement. *Appl. Sci.* **2024**, *14*, 4971. <https://doi.org/10.3390/app14124971>

Academic Editor: Paulo Santos

Received: 11 May 2024

Revised: 3 June 2024

Accepted: 4 June 2024

Published: 7 June 2024



**Copyright:** © 2024 by the authors. Licensee MDPI, Basel, Switzerland. This article is an open access article distributed under the terms and conditions of the Creative Commons Attribution (CC BY) license (<https://creativecommons.org/licenses/by/4.0/>).

## 1. Introduction

Under the influence of urban development, population growth, and traffic congestion, as well as strict control over road excavation by large and extra-large cities, extensive excavation operations are subject to numerous restrictions. Consequently, trenchless jacking technologies are increasingly being applied in urban areas. In jacking engineering, the caisson plays a crucial role as an ancillary structure, due to its high rigidity and good overall integrity. However, it is typically not dismantled after jacking construction is completed. Direct abandonment can lead to resource waste; thus, secondary utilization aligns more closely with the concept of urban sustainable development. The stability of caissons during the operational phase is primarily influenced by fluctuations in groundwater levels due to their relatively deep burial depth. Changes in the service environment and hydrogeological conditions during both construction and operation phases may cause soil non-compaction and local soil slippage. Moreover, the caisson structure itself may experience horizontal tilting, all of which can have unpredictable effects on the stability of the caisson structure.

Yea et al. [1] investigated empirical estimation methods for the unit frictional resistance of large caissons, revealing a reduction in unit frictional resistance with increasing depths of submersion. Song et al. [2] examined the soil deformation mechanisms during caisson construction in dry sand, suggesting that larger shaft diameters can mitigate surface minimal displacement. Wang et al. [3] studied the migration patterns of soil components and elucidated the mechanisms of stratum response patterns. Jiang et al. [4] investigated the behavior of large deepwater caissons in sand, indicating that the distribution pattern of blade resistance is related to burial depth, mud surface height, and submersion status, with stress concentration occurring near the corners of rectangular caissons. Sheil et al. [5] investigated the creation of enlarged foundations by wellbore expansion to provide undrained uplift resistance, demonstrating significant impacts of the cone angle on uplift bearing capacity and horizontal resistance. Liu et al. [6] studied the mechanical characteristics of caissons in soft soil layers. Chen et al. [7] established a mechanical model for caisson submersion, derived the kinematic equations for the caisson process, and revealed the kinematic characteristics and influencing mechanisms of caissons. Wang et al. [8] discovered a three-stage distribution of sidewall frictional resistance of caissons and investigated its distribution mechanism using limit analysis theory. Dong et al. [9] proposed a method for calculating end resistance considering the morphology of caisson blades. Sun et al. [10] proposed a corrective method for significant inclinations of large circular caissons in collapsible loess areas, achieving satisfactory correction results in practice. Zhu et al. [11] conducted centrifuge model tests (100 g) to investigate the vertical and horizontal bearing characteristics of caissons in clay; the findings reveal that cyclic loading markedly improves the horizontal bearing capacity of the caissons, evident in both the load-displacement response and the evolution of soil pressure and pore pressure. Wang et al. [12] proposed that the bearing capacity under lateral loading significantly influences the regular operation of caissons. Employing numerical methods, the horizontal bearing characteristics of caissons and optimized reinforcement schemes were analyzed. Wang et al. [13] developed an Abaqus6.14 model for reinforced concrete piles surrounding caissons to examine the extent and magnitude of deformation in the top caisson and surrounding soil subjected to the jacking force.

The aforementioned studies primarily focused on the stress analysis and corrective measures during caisson construction, with limited reports on the structural stability during long-term operation and no consideration of various adverse factors that may affect caisson performance post construction. It is noteworthy that large-diameter pipe jacking caissons, with their larger cross-sectional and load-bearing areas, face greater technical challenges in terms of load-bearing capacity, lateral force resistance, and deformation under load. This paper investigates large-diameter caissons in the Jinshui River flood control project in Zhengzhou, China. The mechanical behavior of caisson structures and surface subsidence were monitored, and the impact of fluctuating groundwater on structural stability during operation was analyzed using a validated FE method. Considering potential engineering issues such as loose surrounding soil, voids, and caisson inclinations during construction and operation, the effects of these factors on caisson stress and displacement patterns were analyzed. The suitability of permeable polymers, foam polymers, and anchor reinforcement techniques was assessed, along with the structural stability of reinforced caissons during operation.

## 2. Project Overview

The Jinshui River flood control project in Zhengzhou comprises dual-line underground jacking engineering spanning 5.44 km, featuring seven receiving wells and eight working wells along its route, as illustrated in Figure 1. The caissons are constructed with circular reinforced concrete structures with an outer diameter of 12.0 m, an inner diameter of 10.0 m, and a height of 28.85 m, divided into three sections with respective heights of 10.0 m, 9.15 m, and 9.70 m from crown to invert. The invert of the caisson is equipped with a 2.0 m high blade, with a tread width of 0.40 m, utilizing self-weight for undrained excavation.



Figure 1. Caisson alignment along the Jinshui River.

According to the engineering geological survey report, the strata where the caissons are situated consist of miscellaneous fill soil, loess-like light silty soil, and loess-like medium silty soil from top to bottom. These soils exhibit moderate collapsibility, with the groundwater level being 5.66 m above the bottom of the well. The material parameters for the soil and relevant caisson structures are listed in Tables 1 and 2, respectively.

Table 1. Physical and mechanical parameters of soil layers.

Soil Layer	Density/ g·cm <sup>-3</sup>	Cohesive Force/ kPa	Angle of Internal Friction/ °	Compression Modulus/ MPa	Permeability Coefficient/ cm·s <sup>-1</sup>	Poisson's Ratio	Layer Thickness/ m
Miscellaneous fill soil	1.72	8.0	10.0	5.4	-	0.30	0~20.7
Loess-like light silty	1.3	14.0	22.4	7.8	1.8 × 10 <sup>-4</sup>	0.22	20.7~30
Loess-like medium silty	1.5	30.5	13.5	7.8	3.0 × 10 <sup>-5</sup>	0.22	Below 30

Table 2. Material parameters of the caisson structure.

	Elastic Modulus/MPa	Poisson's Ratio	Density/ kN·m <sup>-3</sup>
Bottom sealing concrete	2.00 × 10 <sup>4</sup>	0.2	24
Caisson wall and bottom plate	3.00 × 10 <sup>4</sup>	0.2	25
Rebar	2.06 × 10 <sup>5</sup>	0.3	78
Cement soil	15	0.3	23

### 3. Field Monitoring

During the 1:1 prototype test, the safety level of the caisson was classified as Grade I. The monitoring of the horizontal displacement of the surrounding ground, vertical settlement, horizontal displacement along the depth of the caisson walls, and longitudinal strain inside the caisson was conducted. The objective was to constantly assess the stability

of the ground and caisson structure, promptly detect and address any safety hazards, rectify design and construction deficiencies, prepare for subsequent safe constructions, ensure a safe excavation of the caisson, achieve construction informatization, and compare the results with FE simulations to further its validation. Four monitoring points were symmetrically arranged around the caisson, with the overall monitoring layout detailed in Figure 2. To mitigate the influence of temperature fluctuations on strain gauges, corrective measures were taken to compensate for temperature effects during preliminary tests, and sunshade measures were implemented during monitoring.

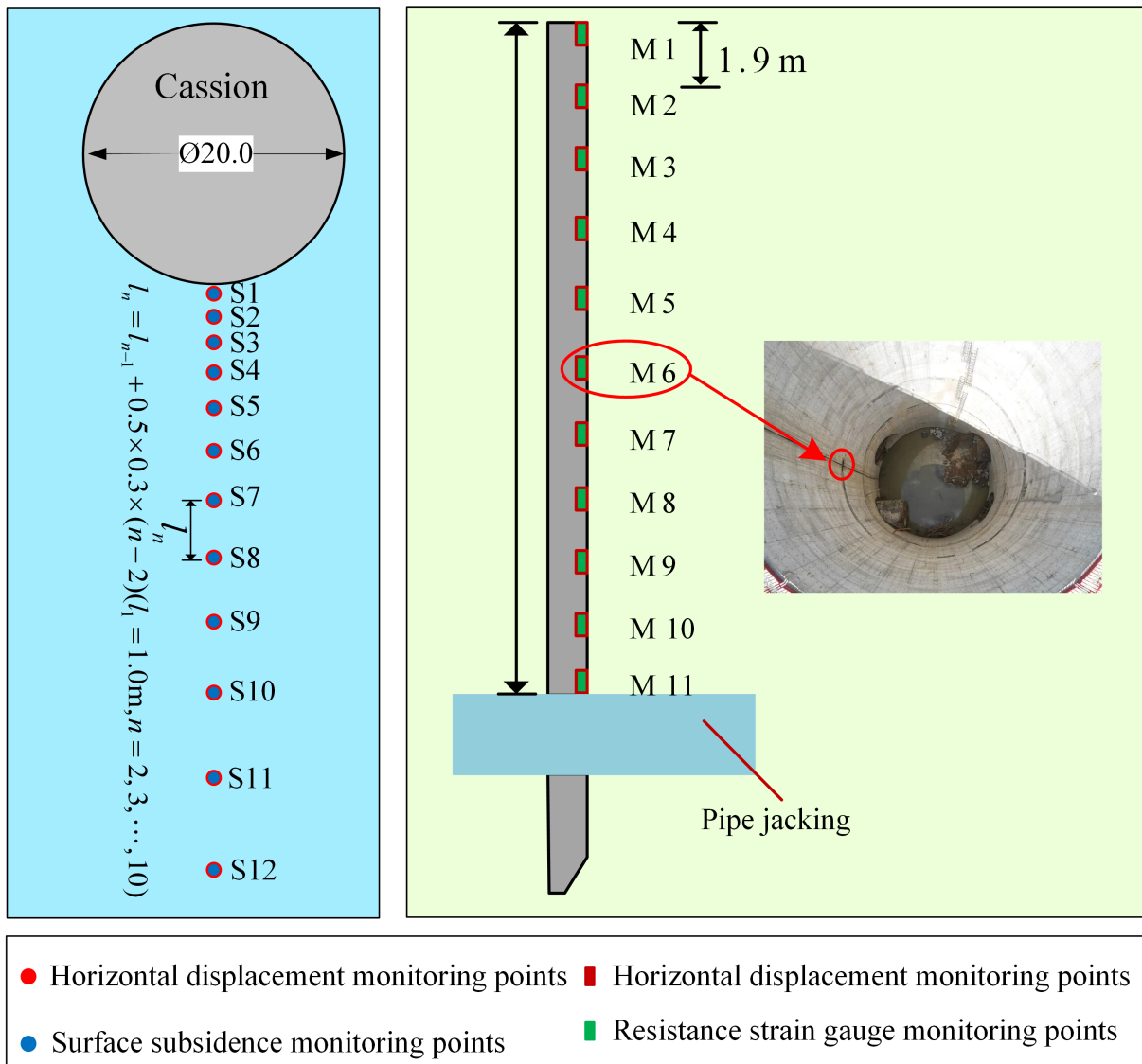


Figure 2. Displacement and strain monitoring at different locations.

#### 4. Finite Element Modeling

##### 4.1. Model Description

The horizontal influence range of the caisson extends to 3.0 times the caisson diameter, while vertically, it reaches approximately 30 m below the bottom of the caisson [14]. Therefore, in the FE model, the long side ( $x$ -axis) of the soil is 144 m, and the short side ( $y$ -axis) is 58.85 m, as shown in Figure 3. To characterize the slipping and separation phenomena at the interface between the caisson and the soil, contact elements were placed at the interface, with a penalty method used for tangential direction [15], a friction coefficient set at 0.4, and hard contact employed in the normal direction. The soil in the model follows the

Mohr–Coulomb yield criterion [16], while concrete structures adopt the concrete damaged plasticity (CDP) model [17]. With the elastic modulus of steel far exceeding that of concrete, it exhibits elastic–plastic behavior before reaching its yield strength and is therefore approximated as a linear elastic material.

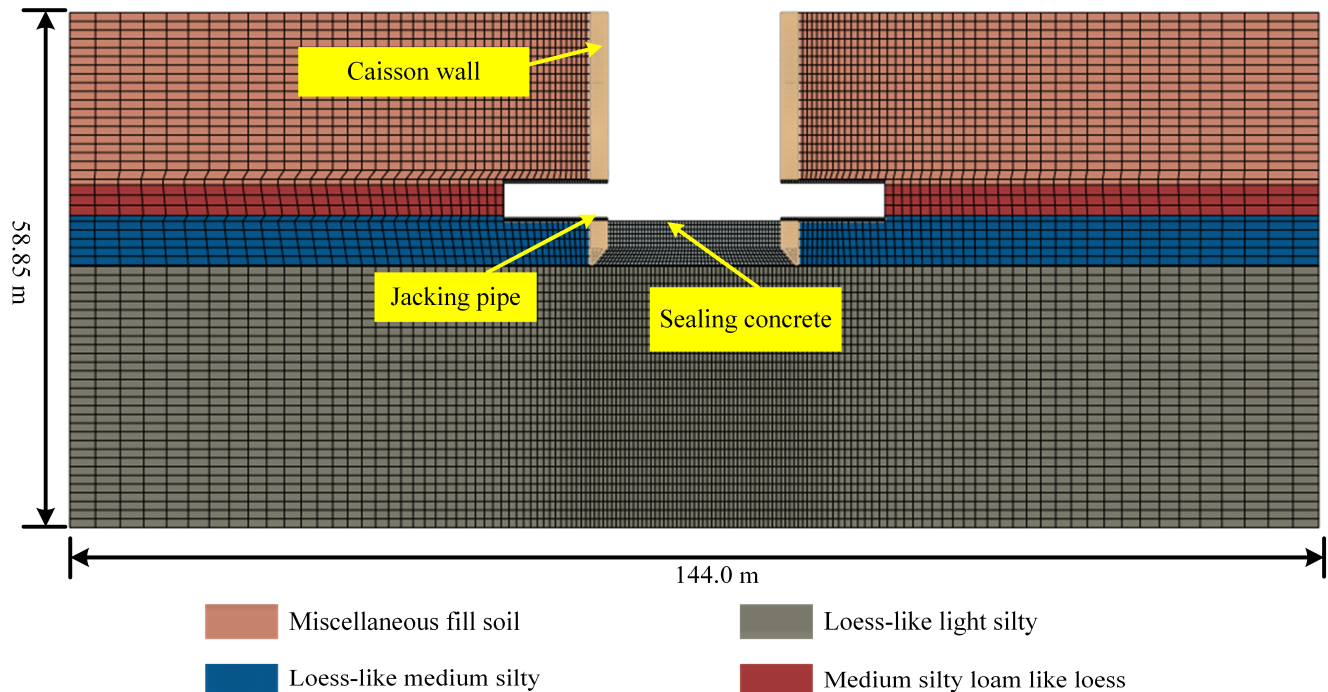


**Figure 3.** FE calculation model of the caisson.

The loess-like light silty soil layer in the model contains a dry–wet separation surface, which acts as a permeable free surface allowing unrestricted settlement with a pore pressure of 0.0. The left and right boundaries constrain horizontal displacements, while the bottom boundary restrains vertical displacements of the soil. The annual fluctuation curve of the groundwater level is simplified into a sinusoidal function. After coding in Fortran2012 programming software, the DISP subroutine was embedded into the FE model to incorporate boundary conditions for calculation. The groundwater fluctuation functions are shown in Equations (1) and (2):

$$P_0 = 10000 \times (-23.19 - y) \quad (1)$$

$$U(1) = P_0 + 10000 \times H \times \sin(\pi t/6) \quad (2)$$

where  $P_0$  is the initial groundwater pressure that varies with burial depth,  $H$  is the amplitude of the annual change in groundwater level, and  $t$  is the time of change in groundwater level (in months).

#### 4.2. Simulation of Caisson Structure Construction Phase

To accurately capture the mechanical behavior of the caisson structure, the initial stress and its distribution during the construction phase were first obtained, serving as the initial state for subsequent simulation conditions. In the simulation, caisson subsidence was achieved by kill-soil elements using the Model Change function and activating caisson structures. The modeling steps strictly followed the on-site construction process, as outlined in Table 3.

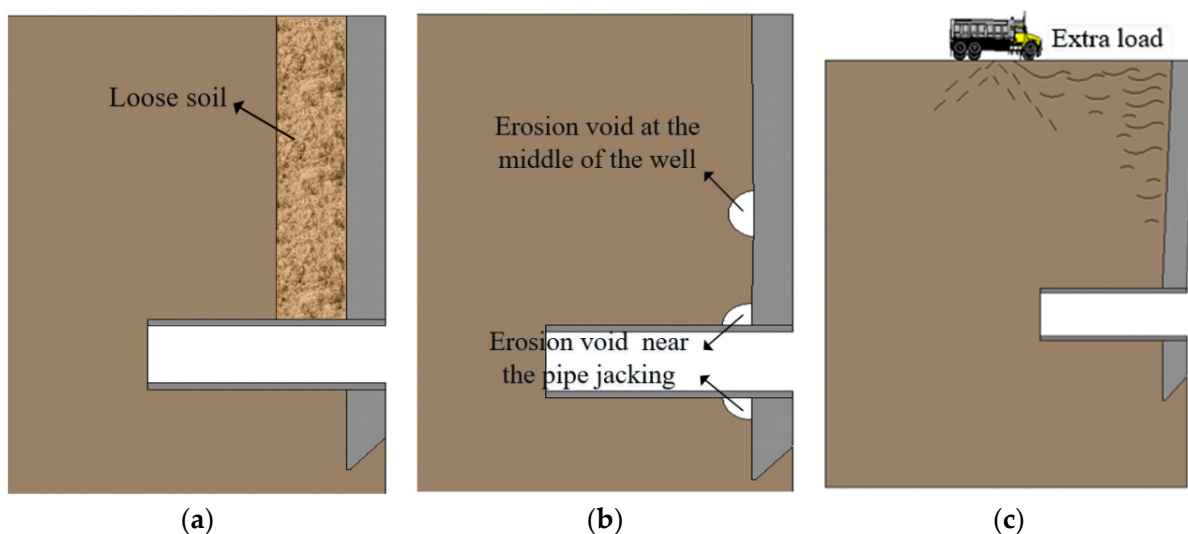
**Table 3.** Model calculation steps.

Steps	Calculation Step
1	'Killing' the caisson structure, performing ground stress equalization and defining the initial stress state.
2	First construction of the caisson: The caisson wall was 'activated', allowing it to settle to a depth of 10.0 m. Simultaneously, the soil inside the excavation pit was 'killed', simulating earthwork excavation.
3	Second construction of the caisson: The caisson wall was 'activated', allowing it to settle to a depth of 19.15 m. Simultaneously, the soil inside the excavation pit was 'killed', simulating earthwork excavation.
4	Third construction of the caisson: The caisson wall was 'activated', allowing it to settle to a depth of 28.85 m. Simultaneously, the soil inside the excavation pit was 'killed', simulating earthwork excavation.
5	Self-compacting concrete was 'activated' to simulate cement sealing.
6	'Killing' the caisson excavation section to simulate the pipe jacking.
7	'Killing' the excavation soil twice, and 'activating' the pipe to complete the 10.0 m pipe jacking construction.

### 4.3. Simulated Conditions

#### 4.3.1. Disease Settings

Surface water infiltration along the caisson wall may result in localized loose soil layers within the insertion depth range, reducing the restraining capacity on the caisson. Under the influence of groundwater fluctuations, the stability of the caisson structure may deteriorate. Various factors during the caisson subsidence process could lead to local soil collapse within the insertion depth range. The leakage of fluid may occur at the intersection of pipes and caissons, causing the loss of fine soil particles with groundwater, leading to long-term erosion and void formation [18]. These voids may gradually increase in size over the years under the influence of groundwater circulation waves, potentially causing instability and damage to the caisson structure. Construction activities such as nearby subways, deep excavations, and pile foundations may impose additional loads on one side of the caisson, resulting in structural tilting on that side. Therefore, investigating the impact of loose soil, erosion voids, and tilting on the stability of caisson structures is of paramount importance. The arrangement of loose soil layers, voids, and tilting defects is illustrated in Figure 4.

**Figure 4.** Schematic diagram of the diseases: (a) loose soil, (b) erosion voids, and (c) tilting.

#### 4.3.2. Reinforcement Methods

To address the effects of loose soil, erosion voids, and caisson tilting on the stability of caisson structures, corresponding reinforcement measures need to be identified. Permeable polymers can penetrate and diffuse into the pores between soil particles, solidifying to reinforce the soil and achieve waterproofing, thereby enhancing soil density and stability. This material effectively mitigates the impact of soil looseness on engineering structures. In the FE model, soil consolidation and reinforcement with permeable polymers were simulated by modifying the field variables in the model, adjusting the modulus of the surrounding soil to simulate soil consolidation, and incorporating the permeable polymer reinforcement.

Foam polymer materials are two-component polyurethane materials that, after absorbing water, expand to form a gel-like substance with high strength and density, bonding with the surrounding soil to fill voids around the caisson [19,20]. In the FE model, voids were filled by “killing” the soil and “activating” the foam polymer material using the Model Change function.

For structural tilting, anchor reinforcement technology was typically employed, transmitting loads through anchor rods to deep soil layers to disperse the load and reduce concentrated loading on the surrounding soil. Therefore, anchor reinforcement technology was chosen in this study to address caisson tilting. The inclination angle of the anchors was set to  $15^\circ$ . In the FE model, the pre-embedded anchor rods were gradually “activated” during the excavation process, anchored to the caisson wall through node coupling, and the influence of variables such as anchor rod size and length on the reinforcement effect was clarified through scenario simulations.

The arrangements for the permeable polymer reinforcement of loose soil, foam polymer filling of voids, and anchor rod reinforcement of tilting are illustrated in Figure 5.

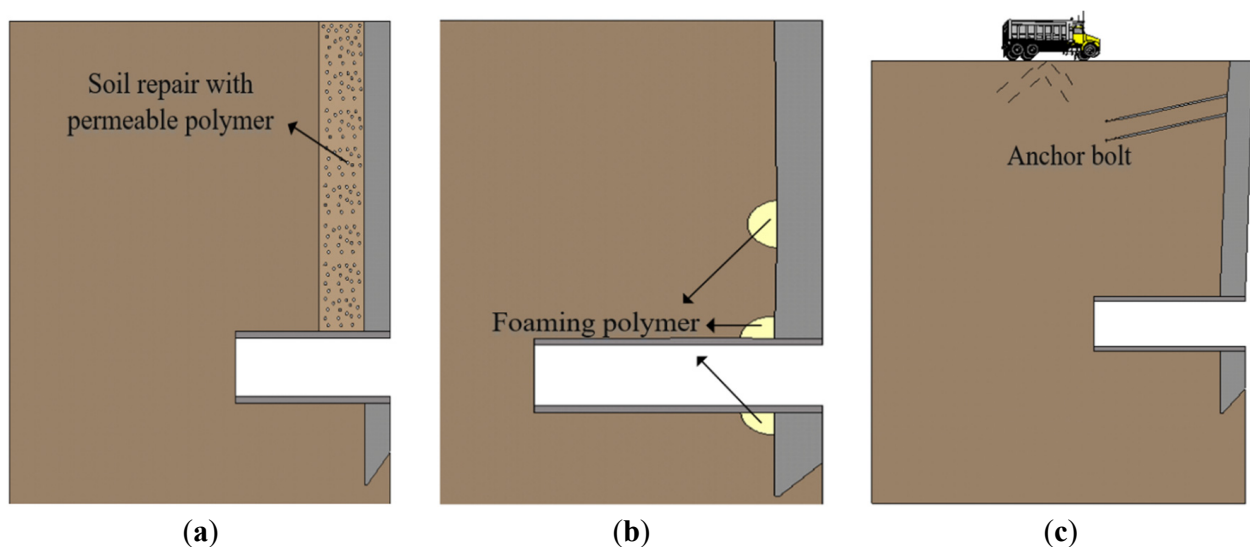


**Figure 5.** Schematic diagram of disease reinforcement: (a) loose soil, (b) erosion void, and (c) tilting.

## 5. Results and Discussion

### 5.1. Comparison between Monitoring and Finite Element Simulation Results

The comparison between the FE simulation and monitoring results of the horizontal displacement and settlement of the ground is illustrated in Figure 6. As shown in Figure 6a, both the monitored and simulated horizontal ground displacements exhibit a nonlinearly accelerating reduction trend as the distance from the monitoring point to the caisson increases. The maximum monitored horizontal displacement is 5.3 mm, while the simulated value is 6.0 mm, resulting in a 13.2% error. Figure 6b demonstrates that the settlement curves of both monitoring and simulation conform to typical characteristics of ground

settlement during excavation, reaching their maximum at monitoring point S3, with a monitored maximum of 3.9 mm and a simulated maximum of 4.3 mm, resulting in an error of 10.2%.

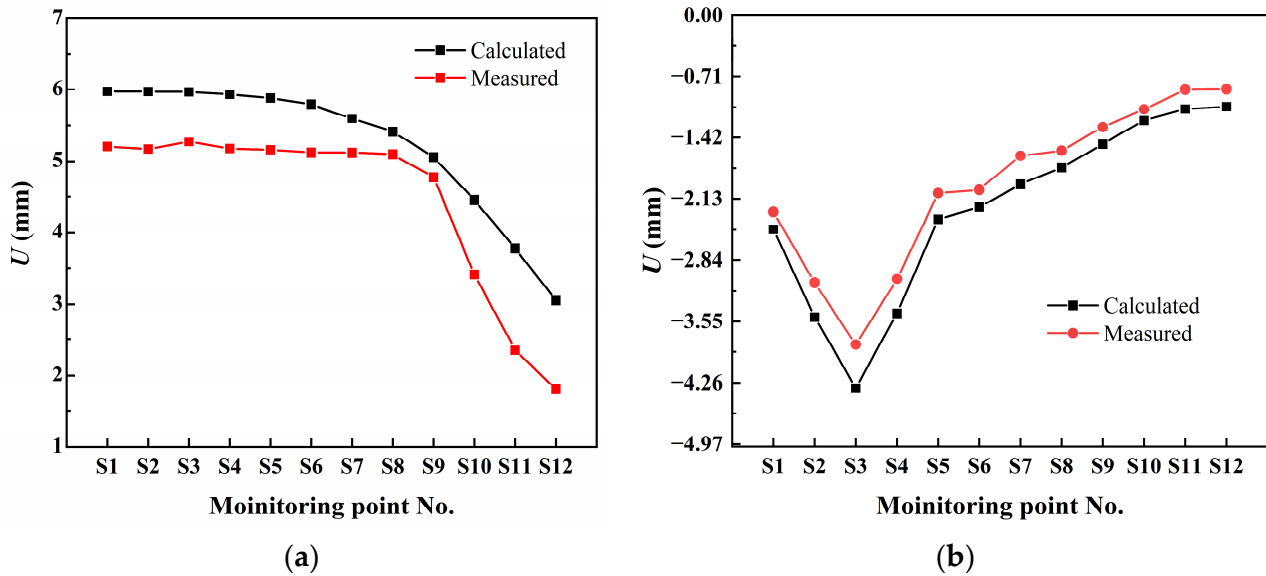


**Figure 6.** Horizontal displacements and vertical settlement of the ground: (a) horizontal displacements and (b) vertical settlement.

The comparison between the FE simulation and monitoring results of the horizontal displacement and longitudinal strain of the caisson is depicted in Figure 7. From Figure 7a, it can be observed that both monitored and simulated caisson horizontal displacements reach their maximum at monitoring point M6, with a monitored maximum of 7.4 mm and a simulated maximum of 7.8 mm, resulting in an error of 5.4%. Figure 7b shows that the longitudinal strain of the caisson increases nonlinearly with depth, and the error between the monitoring and simulation results increases with depth, with a maximum error of 12.5%.

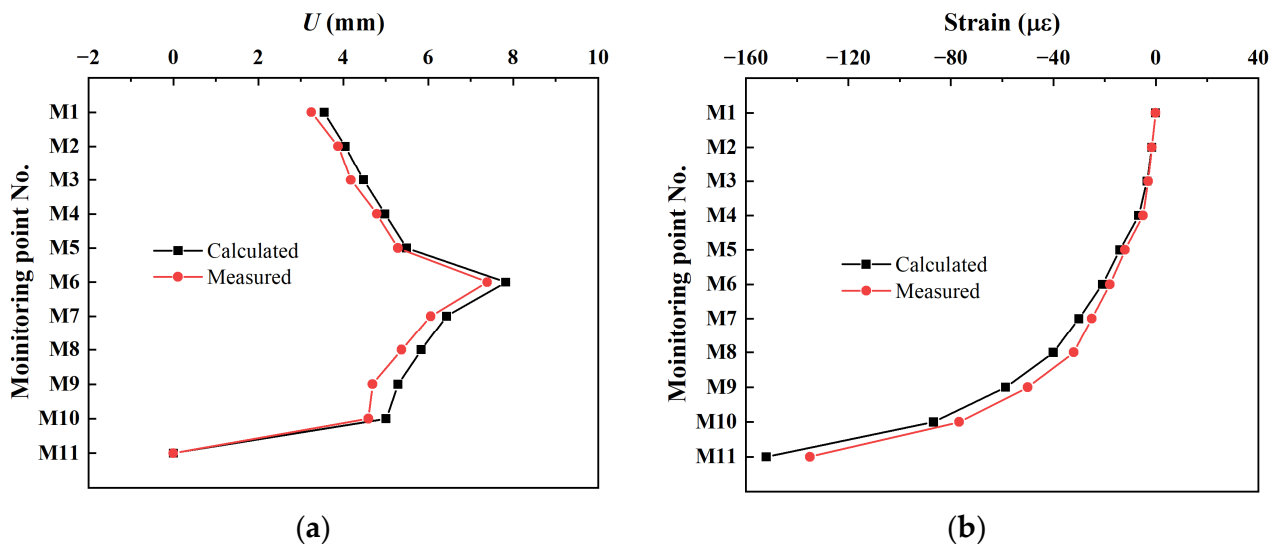


**Figure 7.** Horizontal displacements and longitudinal strains of the caisson wall: (a) horizontal displacements and (b) longitudinal strains.

Overall, the FE simulation results are in good agreement with the prototype test, and the FE simulation tends to be conservative (greater than monitoring values), indicating that the FE model constructed in this study possesses the capability to accurately predict



the mechanical performance of caissons and can provide theoretical guidance for the construction of such caissons.

5.2. Mechanical Behavior of the Caisson Structures during the Construction Phase

Since the reinforced concrete structure is determined based on concrete cracking yield [21], this study employs the maximum principal stress for structural stress analysis. Figure 8 presents the horizontal displacement cloud map of the caisson during construction and the stress distribution curve along its length. It is noted that post construction, the caisson exhibits horizontal displacement towards the excavation pit, with a maximum displacement of approximately 10.0 mm occurring at a depth of one third to half of the excavation pit. This displacement is attributed to stress release during pit excavation, leading to stress redistribution within the caisson. The outward tilting of the outer soil due to active earth pressure towards the interior of the excavation pit contributes to this displacement. In Figure 8b, it is evident that the maximum tensile stress on the caisson wall occurs in the lower outer side of the upper part, reaching a maximum value of approximately 1.47 MPa. The lower part of the caisson wall, functioning as a load-bearing layer under the combined action of cement sealing and earth pressure, exhibits stable behavior and will not be further discussed.

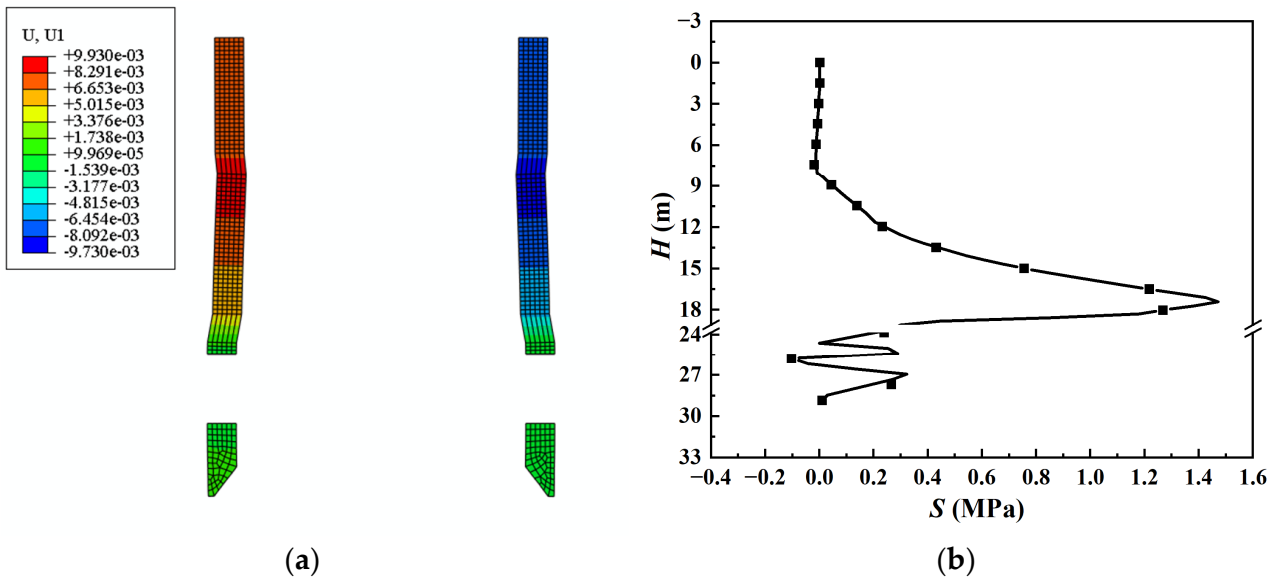


Figure 8. Mechanical behavior of the caisson structure during the construction phase: (a) the horizontal displacement and (b) the distribution curve of the maximum principal stress.

5.3. Influence of Groundwater Fluctuations on the Mechanical Behavior of Caisson Structure

Based on meteorological and hydrological data, the project area receives an average annual precipitation of 677.7 mm. During construction, the groundwater level is situated 23.19 m below the ground and fluctuates seasonally above and below this level. Using the normal water level during construction as a reference, Figure 9 illustrates the horizontal displacement and the maximum principal stress of the upper caisson wall of the jacking pipes, focusing on the outer side of the left caisson wall of the settling well as the pathway. It can be seen that at the annual highest groundwater level (24.86 m), both the horizontal displacement of the upper caisson wall and the maximum principal stress increase. This phenomenon is attributed to the rise in groundwater level, leading to increased pore pressure in the soil and positive pressure at the bottom of the jacking pipes. The jacking pipes experiences upward buoyancy, exerting an upward pressure on the surrounding soil. This causes slight soil deformation, resulting in inward pressure on the upper caisson wall of the jacking pipes. The closer it is to the ground, the greater the displacement. Conversely,

when the groundwater level is at its annual lowest, the stress and the displacement of the caisson wall exhibit the opposite trend.

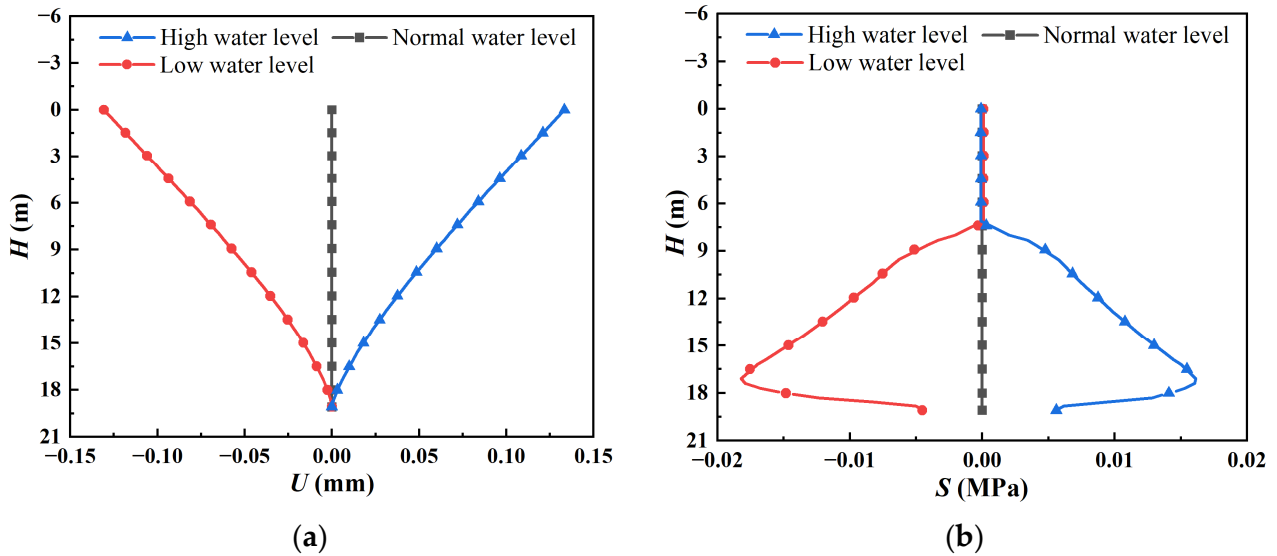


Figure 9. Mechanical behavior of caisson structures under different groundwater levels: (a) the horizontal displacement and (b) the maximum principal stress.

Considering the seasonally fluctuations in the groundwater levels throughout the year, the changes in maximum horizontal displacement and stress of the caisson under seasonal fluctuations for three years were investigated, as shown in Figure 10. It can be observed that after long-term operation, the horizontal displacement changes relatively minimally with groundwater fluctuations, and the seasonal variation in stress remains within the concrete yield cracking range. This indicates that seasonal groundwater variations have minimal impact on the caisson.

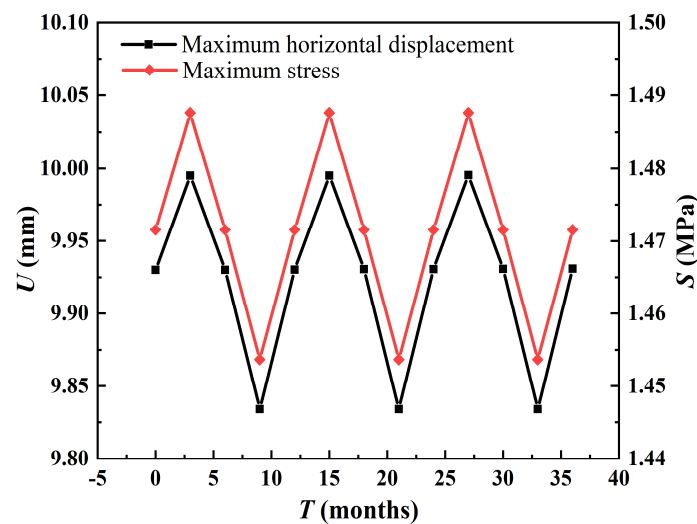


Figure 10. Maximum horizontal displacement and stress of the caisson structures under multiple water level fluctuations for 3 years.

#### 5.4. Mechanical Behavior of Caisson before and after Loose Soil Reinforced Using Permeable Polymer

The soil above the caisson is categorized as miscellaneous fill soil, exhibiting an elastic modulus of 37.8 MPa. Assuming this modulus represents dense soil, the soil with elastic moduli of 30 MPa, 15 MPa, and 5 MPa is considered to be loose and very loose soil,

respectively. The calculated results indicate that with increasing looseness, the settlement of the surrounding soil is 5.67 mm, 8.28 mm, and 11.39 mm, which are 1.31 times, 1.92 times, and 2.63 times the settlement under dense soil conditions (4.32 mm).

As the left-side soil of the caisson undergoes subsidence and collapse, the unbalanced force causes the well to shift to the left. Considering the outer side of the left caisson as the path, with the settlement of the dense soil as the reference, the relative horizontal displacement and stress at different soil density along this path were extracted. As shown in Figure 11a, the maximum tilting of the caisson under the different soil density of loose soil is 0.65 mm, 1.0 mm, and 2.05 mm, respectively. The greater the looseness, the more severe the deformation towards the loose side of the caisson. Meanwhile, due to the restriction of the caisson on the bottom displacement of the jacking pipes, the deformation curvature in the middle of the caisson decreases as the soil becomes less dense. The position with the maximum displacement changes from the middle of the caisson to the upper part.

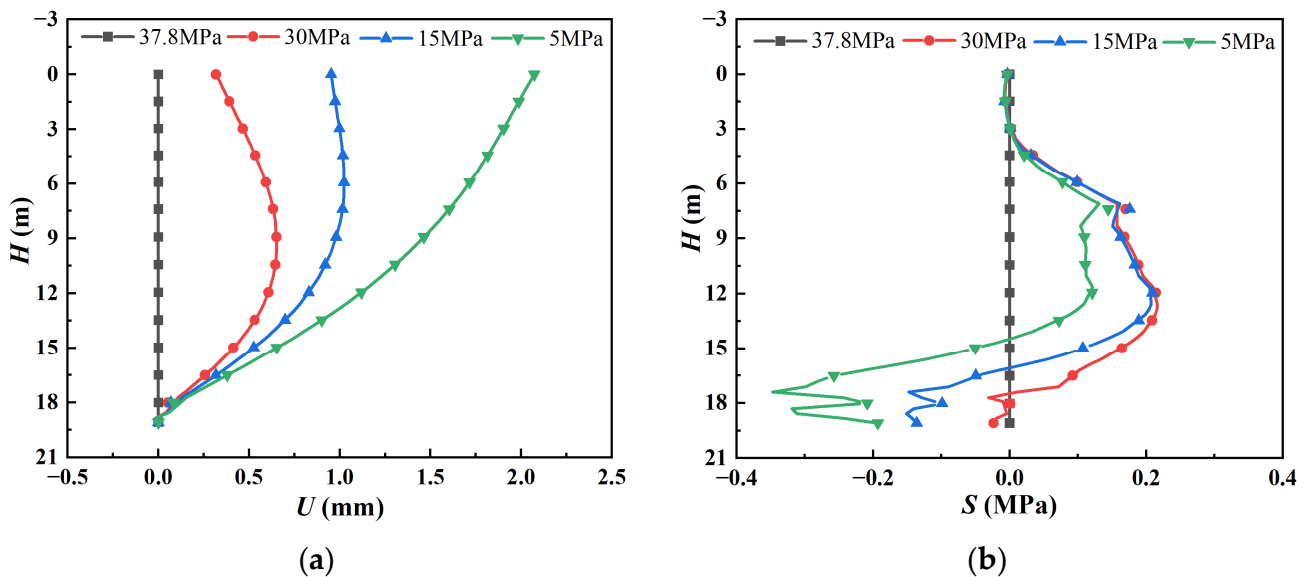


**Figure 11.** Mechanical behavior of caisson structures with different soil densities: (a) the horizontal displacement and (b) the maximum principal stress.

As illustrated in Figure 11b, the bottom concrete structure compresses due to inclined deformation, resulting in higher compressive stress. In the middle of the caisson, deformation increases tensile stress due to soil constraint. However, as soil density decreases, the constraint weakens, reducing tensile stress. When soil modulus decreases from 15 MPa to 5 MPa, the most significant decrease in tensile stress is 0.1 MPa.

A permeable polymer has the ability to infiltrate the pores of the soil, consolidating it and enhancing the density and strength of the soil. The soil strength increases by approximately 2.8 times after reinforcement [22]. The density, elastic modulus, Poisson’s ratio, and permeability coefficient of the permeable polymer material used in this study were  $1.1 \text{ g}\cdot\text{cm}^{-3}$ , 10 MPa, 0.3, and  $7.42 \times 10^{-7} \text{ cm}\cdot\text{s}^{-1}$ , respectively.

Using the loose soil with an elastic modulus of 15 MPa as an example, the elastic modulus of the soil after permeable polymer grouting increases to 57 MPa. A comparison of the caisson’s maximum horizontal displacement and stress before and after reinforcement was conducted, as shown in Figure 12. It is evident that the leftward inclination trend of the caisson is effectively mitigated after reinforcement. Furthermore, owing to the small mass density of the permeable polymer, the grouting expansion not only enhances the strength of the soil but also reduces the inward lateral pressure of the soil on the caisson compared to dense soil, resulting in more effective repair effects.

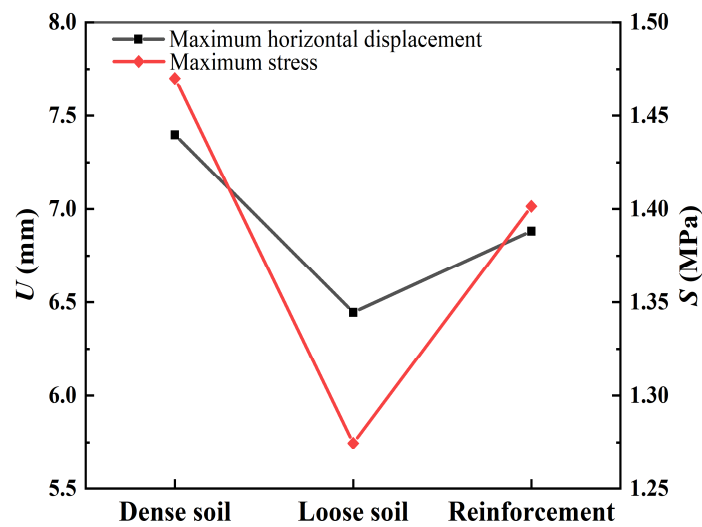


**Figure 12.** Comparison of mechanical behavior of caisson structures before and after reinforcement.

### 5.5. Mechanical Behavior of Caisson before and after Void Filling Using Foamed Polymer

As a consequence of the extreme condition of void formation, the primary impact on the mechanical behavior of the caisson is the removal of soil support at the void location, leading to an uneven distribution of loads around the caisson wall.

Empirical evidence suggests that the depth of the void has a relatively minor effect on the mechanical behavior of the caisson, so it is uniformly set at 0.5 m for analysis. To investigate the influence of void location and size on the structural behavior of the caisson, the middle part of the caisson was selected as the path for void lengths of 2.0 m, 3.0 m, and 4.0 m. A comparison chart of the caisson's mechanical behavior before and after void formation is shown in Figure 13. From Figure 13a, it can be observed that the further the caisson wall from the bottom, the greater the displacement variation, with the maximum displacement located at the crown of the wall. For the void lengths of 2.0 m, 3.0 m, and 4.0 m, the horizontal displacements at the crown of the caisson wall are 0.46 mm, 0.52 mm, and 0.65 mm, respectively. This indicates that within a certain range, a larger void size leads to a greater curvature of the caisson wall from the support layer to the upper part of the void area, resulting in a more severe impact on the stability of the caisson. The curvature decreases in the shallow soil layers, but the deflection continues to increase, and even soil separation may occur. After the occurrence of void formation behind the wall, the stress distribution in the soil layer changes, leading to alterations in the stress experienced by the caisson wall. As shown in Figure 13b, after significant deformation occurs in the upper part of the caisson wall, the wall in the void area is directly affected by the lack of soil constraint, resulting in increased tensile stresses of 0.07 MPa, 0.12 MPa, and 0.34 MPa compared to the intact soil.

Figure 14 presents a comparison of the mechanical behavior of the caisson at different void positions with a void length of 2.0 m in the scenario where void formation occurs at the interface between the jacking pipes and the caisson. As shown in Figure 14a, the maximum displacement at the crown of the caisson wall reaches 1.23 mm, which is 2.4 times that observed for the void located in the middle. It demonstrated that with the same void length, voiding at lower positions, results in more severe damage to the caisson. Furthermore, as illustrated in Figure 14b, an increasing burial depth results in the gradual compression of the caisson. This phenomenon arises because the lower void position contributes to a rise in the self-weight of the soil above the void, subjecting the caisson to lateral soil pressure greater than the tensile stress during deformation. Additionally, the caisson wall in the void area, lacking soil constraint, undergoes tension with a stress of approximately 0.30 MPa.

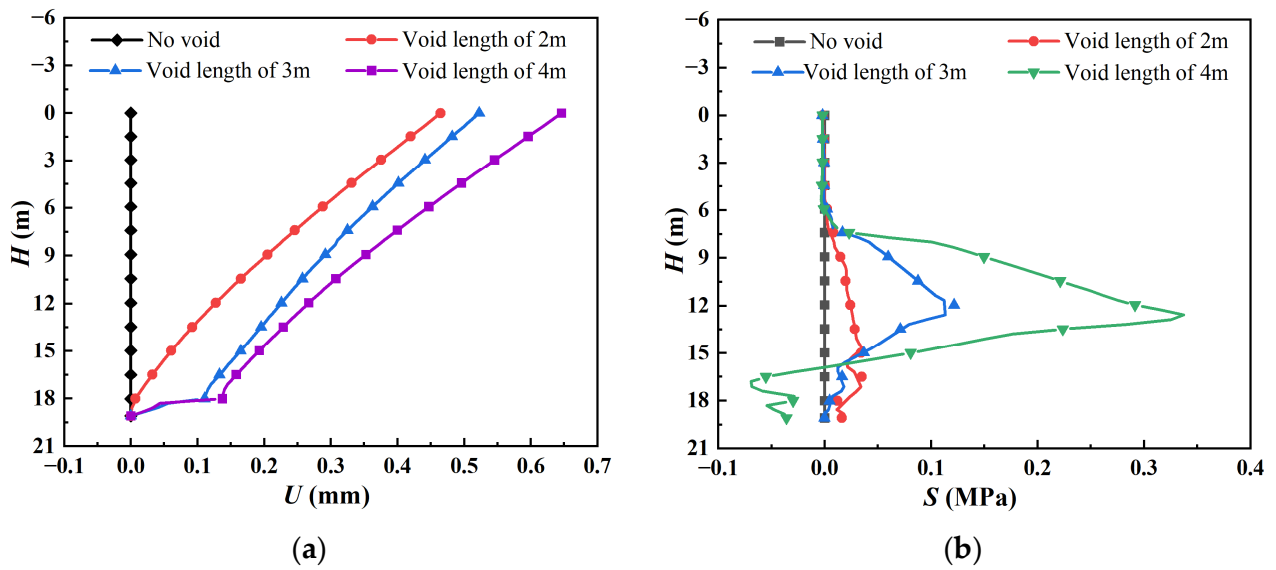


**Figure 13.** Mechanical behavior of the caisson structures with different void length: (a) the horizontal displacement and (b) the maximum principal stress.

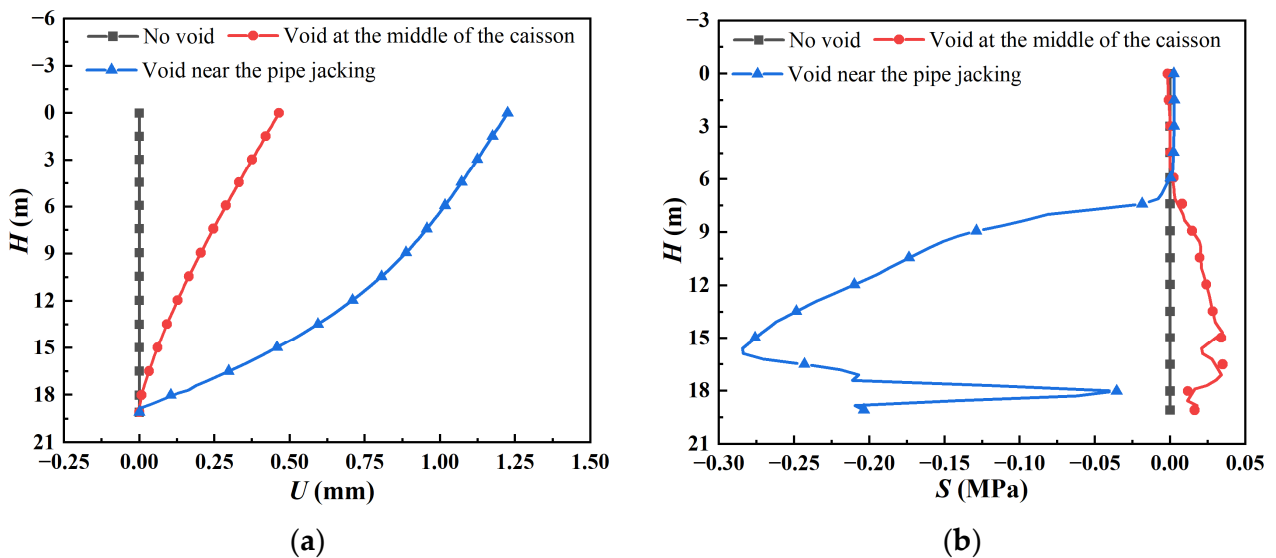


**Figure 14.** Mechanical behavior of caisson structures with different void locations: (a) the horizontal displacement and (b) the maximum principal stress.

The foamed polymer grouting material was designed to expand and fill the void. Given the relatively shallow void position in the middle of the caisson, its impact on the mechanical behavior of the caisson wall is less significant. To prevent polymer expansion from exerting pressure on the caisson wall, a low-density foam-type polymer material was employed to fill this void. Conversely, the void near the jacking pipes is deeper, necessitating a higher-strength filling material to resist soil pressure. Additionally, to minimize leakage, the void area near the jacking pipes was filled using low-exothermic polymer grouting material, thereby reducing the chemical impact of polymer reactions on the caisson and jacking pipes. The density, elastic modulus, and Poisson’s ratio of the low-density polymers are  $0.15 \text{ g}\cdot\text{cm}^{-3}$ ,  $50.0 \text{ MPa}$ , and  $0.2$ , and those of the low exothermic polymers are  $0.30 \text{ g}\cdot\text{cm}^{-3}$ ,  $130.0 \text{ MPa}$ , and  $0.17$ , respectively.

To evaluate the efficacy of different polymers in filling voids, a comparison was made between the horizontal displacement and stress of the caisson, as illustrated in Figure 15. Upon the polymer grouting and expansion filling of the void, the upper part received

polymer support, thereby enhancing soil stability and gradually reducing lateral pressure on the caisson. Consequently, an outward expansion trend of the caisson was observed. When repairing the middle section of the caisson post void formation, as depicted in Figure 15a, the inward inclination is effectively alleviated, and the maximum horizontal displacement at the crown after filling decreases by 0.33 mm. Tensile stress resulting from caisson deformation is also diminished, essentially restoring the stress state to that before void formation and effectively mitigating instability caused by voids. From Figure 15b, it can be observed that the maximum horizontal displacement point decreased by 0.22 mm, gradually stabilizing the caisson and effectively addressing damage from casing voids. Additionally, the lower mass density of the polymer material, to some extent, reduced the lateral pressure exerted by the soil layer, thereby reducing the bending deformation of the caisson.

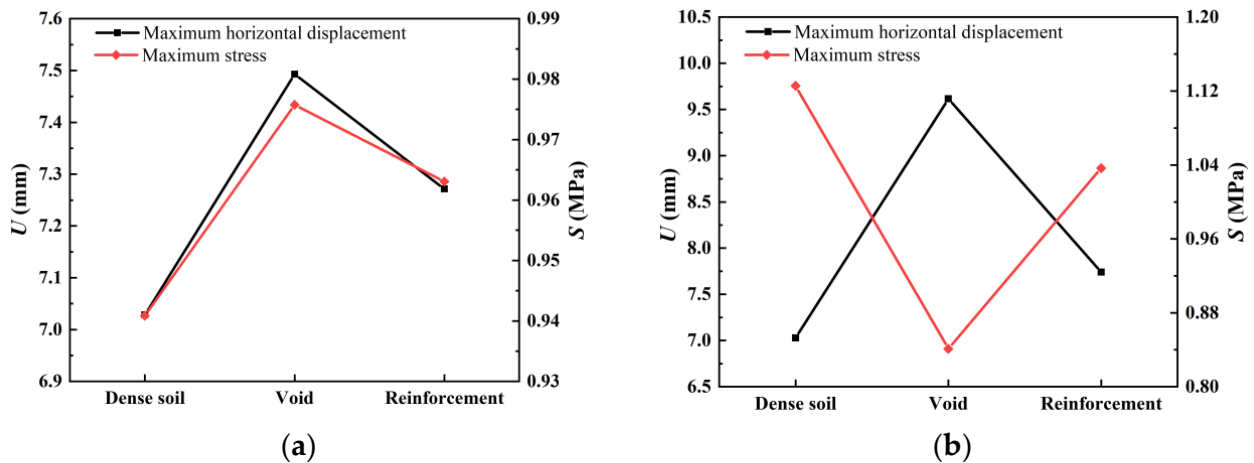


**Figure 15.** Comparison of mechanical behavior of caisson structures before and after filling: (a) void at the middle of the caisson and (b) void near the pipe jacking.

5.6. Mechanical Behavior of Caisson before and after Tilting Anchored

To investigate the impact of tilting on the structural damage of the caisson, tilted loads of 0.05 MPa, 0.10 MPa, and 0.15 MPa were selected for calculation. Figure 16 shows the calculation contour map of the caisson under tilted loads. It can be observed that due to the relief and dissipation of external loads by the soil, the horizontal displacement of the caisson gradually decreases from shallow to deep after being subjected to tilted loads, and the position of the maximum stress also shifts. When there is no tilting, the maximum tensile stress occurs at the maximum deformation of the lower part of the caisson wall, with a value of approximately 1.47 MPa. As the tilting increases, the point of maximum tensile stress shifts to the intersection of the right caisson wall and the pipe jacking. This is because when the left side of the caisson is tilted, the entire structure is subjected to a moment, which causes the lower right pipe to bear a greater stress. Tilting changes the position of the structure’s center of gravity, causing the lower right pipe to bear a greater tilted moment, leading to the maximum stress change.

To explore the mechanical behavior of the caisson under different tilted loads, a comparison was made between the horizontal displacement and the maximum stress of the caisson wall. From Figure 17, it can be seen that with the increase in tilted loads, the maximum horizontal displacements of the caisson wall are 16.31 mm, 27.39 mm, and 50.18 mm, marking respective increases of 2.3 times, 3.7 times, and 6.8 times compared to those under without tilted load conditions. Correspondingly, the maximum tensile stresses register 2.07 MPa, 2.57 MPa, and 2.78 MPa, reflecting respective increments of 1.4 times, 1.7 times, and 1.9 times compared to those under no tilted load. The rate of growth gradually diminishes with the escalating tilted loads, attributed to the fact that while initial stress growth might be rapid upon the application of tilted loads, subsequent internal deformation and compaction occur, gradually unveiling the nonlinear characteristics of

concrete. Consequently, the response of the caisson wall to external loads slows down, resulting in a gradual reduction in the stress growth rate.

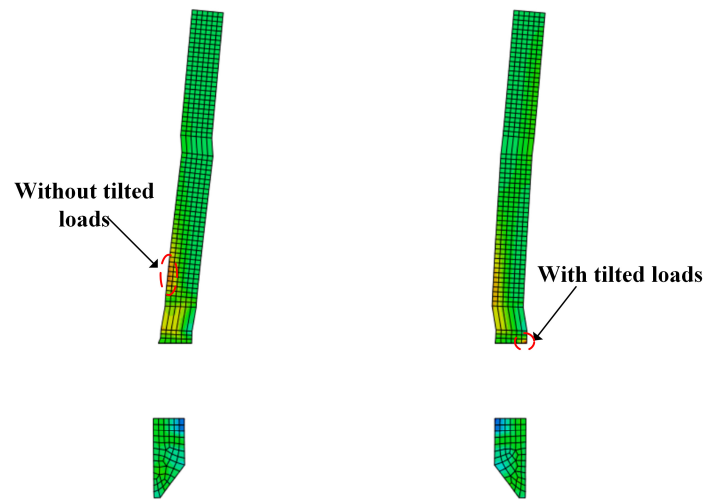


Figure 16. Calculated cloud for caisson under tilted loads.

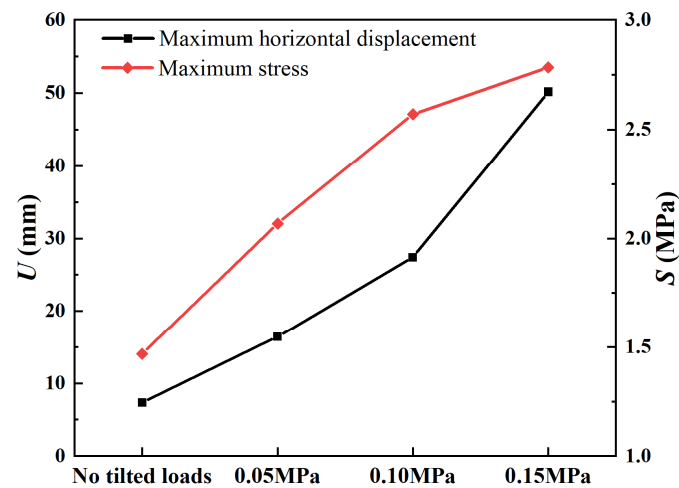
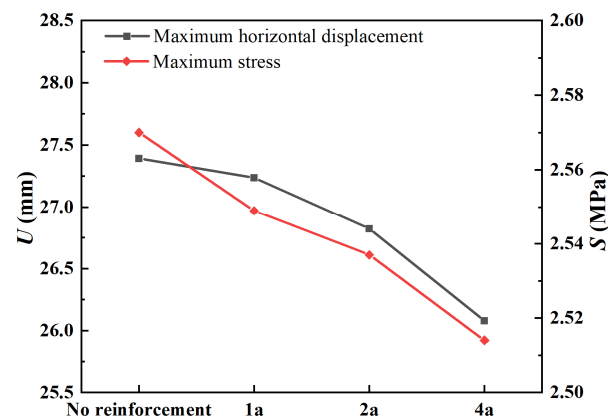


Figure 17. Comparison of mechanical behavior of caisson under different tilted loads.

The tensile capacity of anchor rods is much higher than that of the foundation materials. Pre-embedded anchor rods can increase the overall stiffness of the foundation, making the foundation structure more stable and effectively reducing the structural damage caused by tilted loads. We use the method of controlling variables to explore the influence of the cross-sectional area and length of the anchor rod on the reinforcement effect when the tilted load is 0.1 MPa.

When the length of the anchor rod is 20 m, the cross-sectional size of the anchor rod gradually increases to 1a, 2a, and 4a ( $a = 2.1 \text{ cm}^2$ ). Figure 18 shows a comparison of the mechanical behavior of the caisson under different anchor rod cross-sections. It can be seen that as the cross-sectional area of the anchor rod increases, the relative horizontal displacement of the caisson without anchoring is reduced by 0.15 mm, 0.57 mm, and 1.32 mm, respectively, and the maximum tensile stress of the caisson is reduced by 0.021 MPa, 0.033 MPa, and 0.056 MPa, respectively. The ability to resist deformation under the same tilted load becomes stronger. This is because the increase in the cross-sectional area of the anchor rod increases the friction between the anchor rod and the surrounding soil or rock layers, making it more difficult for the anchor rod to be pulled out or slide, while also being able to bear more load, reduce the impact of the load on the structure, and enhance the stability and bearing capacity of the structure.



**Figure 18.** Comparison of mechanical behavior of caisson structures with different anchor cross-sections.

When the cross-sectional area of the anchor rod is 2a, the lengths of the anchor rods gradually increases to 15 m, 20 m, and 25 m. Figure 19 shows a comparison of the mechanical behavior of the caisson under different anchor rod lengths. It can be seen that with the increase in the anchor rod length, the maximum horizontal displacement of the caisson is reduced by 0.38 mm, 0.57 mm, and 0.73 mm, respectively, and the maximum tensile stress is reduced by 0.021 MPa, 0.033 MPa, and 0.056 MPa, compared to the condition of no anchoring. This highlights the superior anchoring effect of longer anchor rods on the caisson. The rationale behind this lies in the increased distance between connection points facilitated by longer anchor rods. Consequently, longer anchor rods offer enhanced tensile strength, thereby fortifying the structure and bolstering its stability and load-bearing capacity.

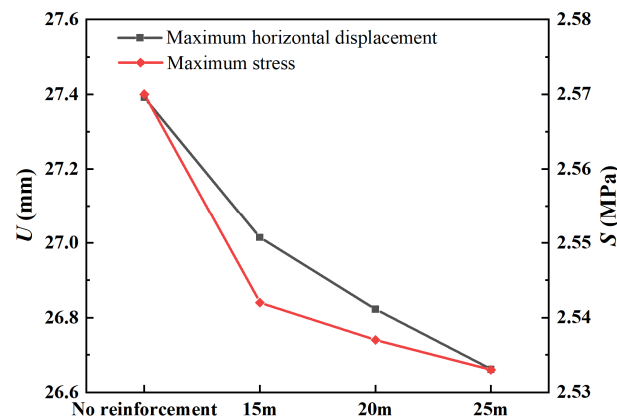


**Figure 19.** Comparison of horizontal displacement of the caisson structures with different anchor lengths.

## 6. Conclusions

Based on the Jinshui River flood control project in Zhengzhou City, the impact of groundwater fluctuations on the stability of super-large-diameter caisson structures under normal conditions, loose soil, void, and tilted structures were analyzed. The applicability and enhancement effects of permeable polymer, foam polymer, and anchor technologies in loose soil, voids, and tilted caissons were discussed. The following conclusions are drawn:

1. Post construction, the caisson exhibits horizontal displacement towards the excavation pit, with a maximum displacement of approximately 8.0 mm occurring at a depth of one third to one half of the excavation pit, showing a trend of small at both ends and large in the middle. With the concrete bottom filling the excavation space and increasing the support force of the soil, the settlement and deformation of the soil are reduced.



2. Seasonal groundwater fluctuations with relatively small amplitudes do not induce significant displacements and stresses changes in the caisson structure. The maximum displacement and stress in the caisson caused by groundwater fluctuations are measured at 0.14 mm and 0.017 MPa, respectively.
3. With the increase in soil looseness, the maximum deformation of the caisson reaches 2.05 mm. The reduction in tensile stress is most significant when the soil's elastic modulus decreases from 15 MPa to 5 MPa. The use of permeable polymer grouting can significantly enhance the soil's compaction and bearing capacity, thereby strengthening the structural stability of the caisson.
4. Soil voids markedly alter stress distribution within soil layers. A void length of 4.0 m leads to a 41% greater caisson deformation compared to a void length of 2.0 m. Voids near the jacking pipes induce a maximum displacement that is 2.4 times greater than the displacement induced by those located in the middle of the caisson. Larger void sizes and lower void positions adversely impact caisson structural stability. The use of foam polymer materials effectively mitigates these adverse effects.
5. Tilted loads induce significant deformation in the caisson. With a tilted load of 0.15 MPa, the maximum horizontal displacement of the caisson is 6.8 times larger than that without a tilted load. Anchoring mitigates damage from inclined loads, with effectiveness improving with larger cross-sectional areas and longer anchor rod lengths.

**Author Contributions:** Conceptualization, B.L.; methodology, L.D. and Y.Y.; investigation, data curation and supervision, H.W.; project administration, D.D. All authors have read and agreed to the published version of the manuscript.

**Funding:** This research was funded by the Postdoctoral Science Foundation of China (No. 2022TQ0305) and the Youth Talent Promotion Project of Henan Province (No. 2023HYTP016), for which the authors are grateful.

**Institutional Review Board Statement:** Not applicable.

**Informed Consent Statement:** Not applicable.

**Data Availability Statement:** The data presented in this study are available in the article.

**Conflicts of Interest:** Author Haitao Wang was employed by the company Zhengzhou Zhengfa Water Conservancy Engineering Company Limited. The remaining authors declare that the research was conducted in the absence of any commercial or financial relationships that could be construed as a potential conflict of interest.

## References

1. Yea, G.G.; Kim, T.H.; Kang, G.C. Assessing Unit Skin Friction of Pneumatic Caissons. *Mar. Georesour. Geotechnol.* **2015**, *33*, 127–134. [[CrossRef](#)]
2. Song, G.Y.; Sheil, B.B. Laboratory Testing of Construction-Induced Ground Displacements for Open Caisson Shafts in Sand. *J. Geotech. Geoenviron. Eng.* **2023**, *149*, 04023086. [[CrossRef](#)]
3. Wang, Y.Z.; Liu, M.B.; Liao, S.M.; Yi, Q.; He, J.; Liu, L.; Gong, Z.; Li, K. Investigation on the Stratigraphic Response and Plugging Effect Induced by Press-In Open Caisson in Mucky Soil. *KSCE J. Civ. Eng.* **2023**, *27*, 1928–1941. [[CrossRef](#)]
4. Jiang, B.N.; Yu, T.; Peng, W.M.; Zhang, Y.B.; He, S.B.; Ma, J.L. Analysis of Mechanism of Sand Gushing and Sudden caisson of Ultra-large Deep-water Open Caisson in sand via Field and Model Tests. *Appl. Ocean. Res.* **2023**, *130*, 103436. [[CrossRef](#)]
5. Sheil, B.B.; Templeman, J.O.; Orazalin, Z.; Phillips, B.M.; Song, G. Undrained uplift resistance of under-reamed open caisson shafts. *Geotechnique* **2023**, 1–42. [[CrossRef](#)]
6. Liu, M.; Sun, F.; Gan, Q.; Chi, E.; Li, X.; Ge, G.J. Mechanical Performance of Deep Circular Caisson in Deep Layered Soft Soil. *Math. Probl. Eng.* **2022**, 2022, 5918374. [[CrossRef](#)]
7. Chen, B.G.; He, J.X.; Luo, R.P.; Zhang, G.H.; Gao, Q. Kinematic characteristics and caisson control of open caisson during caisson process. *Rock Soil Mech.* **2022**, *43* (Suppl. 2), 425–430+453.
8. Wang, J.; Liu, Y.; Zhang, Y. Model test on sidewall friction of open caisson. *Model Test Sidewall Frict. Open Caiss.* **2013**, *34*, 659–666.
9. Dong, X.C.; Guo, M.W.; Jiang, Z.X.; Wang, S.L.; Chen, Z.W. End Resistance Calculation and Analysis of Super-Large Open Caisson During Soil Excavation caisson Based on Monitored Soil Pressure Data. *Bridge Constr.* **2022**, *52*, 78–84.

10. Sun, C.L.; Sun, K.; Sun, L.; Ma, X.; Si, D.F.; Wang, X.P. Analysis on Correction of Large Circular Caisson Construction in Collapsible Loess Area. *Constr. Technol.* **2023**, *52*, 10–13.
11. Zhu, B.; Li, Z.Y.; Chen, X.C.; Kong, D.; Qian, H.; Yang, M.; Pan, J.; Zhang, Z. Experimental study on vertical and lateral behaviour of open caisson foundations in clay. *Mar. Georesour. Geotechnol.* **2023**, *41*, 555–565. [[CrossRef](#)]
12. Wang, A.H.; Zhang, Y.F.; Xia, F.; Luo, R.P.; Wang, N. Study of the Lateral Bearing Capacity and Optimization Reinforcement Scheme of an Open Caisson with Consideration of Soil Disturbance. *Appl. Sci.* **2022**, *12*, 5498. [[CrossRef](#)]
13. Wang, Z.X.; Lian, J.Y.; Mao, J.M.; Yang, X.Q.; Song, L.M. Research on Three Dimensional Soil Failure Shape and Settlements Around Shallow Buried Pipe Jacking Caisson. *Tunn. Constr.* **2022**, *42* (Suppl. 1), 257–266.
14. Yi, Q.; Liao, S.M.; Zhu, J.W.; Xu, W. Finite Element Analysis of Soil Squeezing Effect Induced by Press-in Caisson in Muddy Ground. *Tunn. Constr.* **2019**, *39*, 1981–1992.
15. Zhai, K.J.; Zhang, C.; Fang, H.Y.; Ma, H.; Ni, P.; Wang, F.; Li, B.; He, H. Mechanical responses of bell and spigot joints in buried prestressed concrete cylinder pipe under coupled service and surcharge loads. *Struct. Concr.* **2020**, *22*, 827–844. [[CrossRef](#)]
16. Robert, D.J.; Rajeev, P.; Kodikara, J.; Rajani, B. Equation to predict maximum pipe stress incorporating internal and external loadings on buried pipes. *Can. Geotech. J.* **2016**, *53*, 1315–1331. [[CrossRef](#)]
17. Lee, J.; Fenves, G.L. Plastic-damage model for cyclic loading of concrete structures. *J. Eng. Mech.* **1998**, *124*, 892–900. [[CrossRef](#)]
18. Li, B.; Fang, H.Y.; Yang, K.J.; Zhang, X.J.; Du, X.M.; Wang, N.N.; Guo, X.X. Impact of erosion voids and internal corrosion on concrete pipes under traffic loads. *Tunn. Undergr. Space Technol.* **2022**, *130*, 104761. [[CrossRef](#)]
19. Li, B.; Yu, W.; Xie, Y.E.; Fang, H.Y.; Du, X.M.; Wang, N.N.; Zhai, K.; Wang, D.C.; Chen, X.M.; Du, M.R.; et al. Trenchless rehabilitation of sewage pipelines from the perspective of the whole technology chain: A state-of-the-art review. *Tunn. Undergr. Space Technol.* **2023**, *134*, 105022. [[CrossRef](#)]
20. Li, B.; Wang, F.M.; Fang, H.Y.; Yang, K.J.; Zhang, X.; Ji, Y.T. Experimental and Numerical Study on Polymer Grouting Pretreatment Technology in Void and Corroded Concrete Pipes. *Tunn. Undergr. Space Technol.* **2021**, *113*, 103842. [[CrossRef](#)]
21. Li, J.T. Key Techniques for Construction of Open Caissons of Main Ship Channel Bridge of Hutong Changjiang River Bridge. *Bridge Constr.* **2015**, *45*, 12–17.
22. Fang, H.Y.; Liu, K.; Du, X.M.; Wang, F.M. Experiment and numerical simulation of water plugging law of permeable polymer in the water-rich sand layer. *Sci. Sin. Technol.* **2023**, *53*, 457–472. (In Chinese) [[CrossRef](#)]

**Disclaimer/Publisher’s Note:** The statements, opinions and data contained in all publications are solely those of the individual author(s) and contributor(s) and not of MDPI and/or the editor(s). MDPI and/or the editor(s) disclaim responsibility for any injury to people or property resulting from any ideas, methods, instructions or products referred to in the content.